

## BIOTITE ALTERATION IN DEEPLY WEATHERED GRANITE. II. THE ORIENTED GROWTH OF SECONDARY MINERALS

R. J. GILKES AND ANCHALEE SUDDHIPRAKARN<sup>1</sup>

Department of Soil Science and Plant Nutrition, University of Western Australia  
Nedlands, Western Australia, Australia 6009

**Abstract**—Single grain X-ray and electron diffraction patterns of weathered biotite flakes exhibit groupings of 00l and hk reflections of biotite, vermiculite, mixed-layer clay minerals, and kaolinite indicating that the secondary minerals are in parallel crystallographic orientation to the parent biotite. Asterism of biotite reflections is enhanced by weathering. Gibbsite crystals developed in parallel basal orientation to biotite flakes. Most goethite in weathered biotite occurs as aggregates of randomly oriented crystals in cleavages and on grain surfaces. Some goethite is present on micaceous fragments as 0.05- $\mu$ m size, lathlike crystals in a hexagonal arrangement with their (100) face resting on the (001) biotite face. Selected area electron diffraction patterns of aggregates of lathlike goethite crystals contain 0k $\ell$ , 1k $\ell$ , and 2k $\ell$  reflections due to undulation of the aggregates and the extreme thinness of the crystals. These patterns indicate that the close packed anion layers in goethite coincide with the brucite-like layer of the micaceous minerals.

**Key Words**—Biotite, Electron diffraction, Goethite, Orientation, Vermiculite, Weathering products.

### INTRODUCTION

Gilkes and Suddhiprakarn (1979) showed that weathered biotite in saprolite and pallid zone materials formed granular pseudomorphs consisting of various mixtures of biotite, vermiculite, mixed-layer biotite-vermiculite, kaolinite, gibbsite, goethite, and hematite. They found that the abundance of secondary minerals within the grains increased towards the surface of the soil although grains at different stages of alteration were present in each horizon. The mineralogy of these weathering products is similar to that of the altered biotite described by Eswaran and Heng (1976) and Eswaran and Bin (1978), but little information is available in the literature on the mechanism of these transformations.

Single crystal X-ray and electron diffraction techniques have been used to determine how the structure of the parent biotite grains influences the nature and arrangement of weathering products.

### MATERIALS AND METHODS

Altered biotite grains were separated from saprolite and pallid zones of deeply weathered granitic rocks at Jarrahdale, southwest Australia. Details of soil properties and separation procedures are found in Gilkes and Suddhiprakarn (1979).

X-ray diffraction (XRD) patterns of single,  $\sim$ 0.5-mm size flakes were obtained with Fe-filtered cobalt radiation using a Philips 114-mm diameter camera equipped with low angle collimator and beam trap. The flakes were not rotated during exposure and were positioned perpendicular and parallel to the beam for successive

photographs. The mounted flakes were next inserted into a Gandolfi camera (Gandolfi, 1967), and random orientation diffraction patterns obtained to permit identification of all minerals present. Some flakes were given one or more treatments with citrate-bicarbonate-dithionite (CBD) solution to remove goethite. Several flakes of fresh biotite were treated with sodium tetraphenylboron solution to convert them to vermiculite, and XRD patterns were obtained of the products.

Selected area electron diffraction (SAD) patterns were obtained from submicrometer-size grains separated from altered biotite flakes using a Hitachi HU IIB electron microscope. Alteration products and associated mica substrate from freshly cleaved surfaces of altered biotite flakes were dispersed in water and deposited onto carbon-covered grids. A 20- $\text{\AA}$  thick layer of tin was used as an internal standard where accurate measurement of spacings was required.

Some figures showing XRD and SAD patterns have been modified to improve the photographic reproduction of weak reflections and increase resolution of closely adjacent reflections. These features were clearly visible in the original patterns. The notations A5R, etc. in the figures refer to sample horizons. The notation  $\rightarrow \equiv$  and  $\rightarrow \parallel$  is used in figures to signify respectively XRD patterns taken with flakes parallel and perpendicular to the beam.

### RESULTS

#### *X-ray diffraction of single flakes*

Flakes oriented parallel to the X-ray beam gave enhanced basal reflections, and those oriented normal to the beam gave enhanced hk reflections (MacEwan, 1961). Typical XRD patterns for a fresh biotite flake are shown in Figure 1A, B. Both patterns are complex,

<sup>1</sup> Permanent address: Department of Soil Science, Kasetsart University, Bangkok, Thailand.

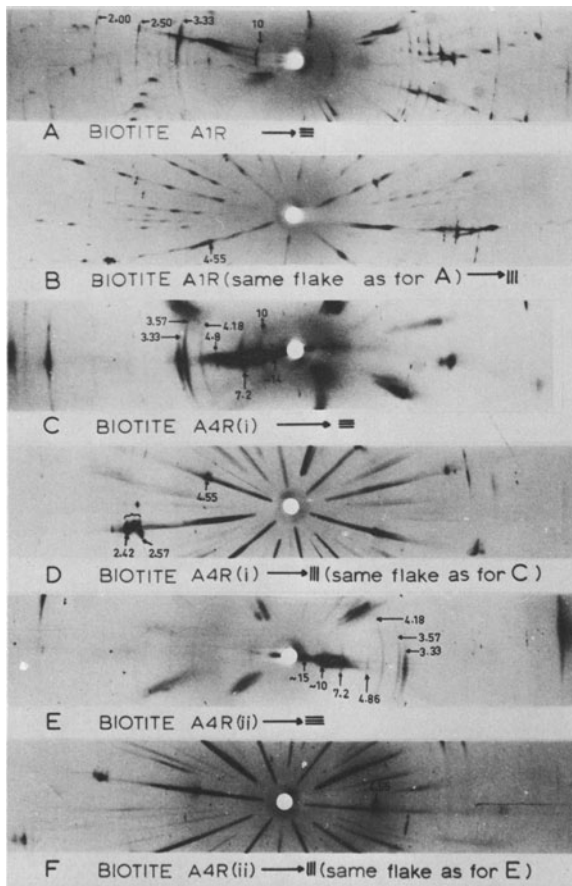


Figure 1. XRD patterns of single biotite flakes taken with the beam parallel ( $\rightarrow \equiv$ ) or normal ( $\rightarrow \parallel$ ) to the stationary flakes. (A, B) Fresh flake from granitic rock. (C, D) Altered flake from saprolite. (E, F) Altered flake from saprolite. Spacings are indicated in Ångstrom units.

containing many hkl Laue reflections. The strong basal reflections at 10, 3.33, 2.50, and 2.00 Å occur on a single axis in Figure 1A. The strong 020 reflections (4.55 Å) occur on continuous streaks in Figure 1B. The streaking of nonbasal reflections (asterism) is a characteristic of biotite and is due to random defects in structure (Hendricks, 1940).

Figures 1C, D, E, and F are patterns of flakes from the saprolite zone which exhibit intermediate stages of alteration. These flakes contain vermiculite and/or mixed-layer mineral (14–15 Å), kaolinite (7.2 Å), gibbsite (4.8 Å), goethite (4.18 Å), and biotite (10 Å). The basal reflections of biotite, vermiculite, mixed-layer clay minerals, kaolinite, and gibbsite are on a single axis in Figures 1C and 1E demonstrating the parallel orientation of these platy minerals within the flake. Goethite gave continuous rings indicating that goethite crystals are not preferentially oriented. The hk reflections of the platy minerals at about 4.5 Å and 2.5 Å fall

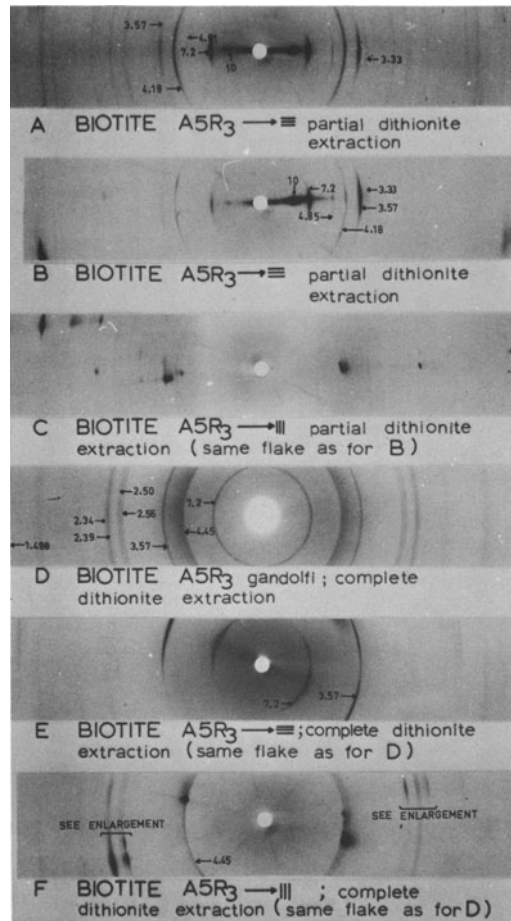


Figure 2. XRD patterns of dithionite (CBD)-treated single flakes of highly altered biotite from pallid zone. Patterns were obtained with the beam parallel ( $\rightarrow \equiv$ ) or normal ( $\rightarrow \parallel$ ) to the stationary flakes or with rotation in a Gandolfi camera. Spacings are indicated in Ångstrom units.

on streaks which have become much more intense with the increased disorder of these minerals due to weathering.

Diffraction patterns characteristic of flakes at an advanced stage of alteration are presented in Figures 2A, B, and C. These flakes contained abundant aluminum-substituted goethite which dominates the diffraction pattern and obscures lines due to other minerals. Partial removal of goethite by CBD treatment permitted identification of other components (biotite 10 Å, kaolinite 7.2 Å, gibbsite 4.85 Å), in parallel orientation. Electron microscopy showed that some goethite crystals within opened cleavages are arranged in hexagonal patterns upon the micaceous substrate (Gilkes and Suddhiprakarn, 1979). Removal of the much more abundant, non-oriented, fine-grained deposits of goethite from the exteriors and highly exfoliated interlayers of flakes by CBD treatment might have permitted detection of pre-

ferred orientation in the remaining interlayer goethite. However, no clear evidence of preferred orientation of goethite was seen in patterns of the CBD-treated flakes. Fluctuations in intensity around the goethite diffraction rings were probably caused by variations in adsorption of the diffracted beam due to the platy morphology of the flakes.

Some highly altered biotite flakes from the pallid zone were repeatedly treated with CBD solution until no goethite remained. The fragile residues usually consisted of various mixtures of biotite, vermiculite, mixed-layer clay minerals, kaolinite, and gibbsite. Some flakes appeared to consist solely of highly oriented kaolinite (Figures 2D and E), but the faint residual asterism (Figure 2F) suggests the presence of minor amounts of micaceous minerals.

In XRD patterns of altered biotite taken with the beam perpendicular to the flakes, the nonbasal hk reflections of micaceous minerals usually occurred on well-defined axes (Figure 2F). The 02 and 11 reflections near 4.5 Å defined the direction of the b-axes. The nature of a series of reflections oriented on an axis 30° to the b-axis, with spacings near 2.5 Å, varied with the relative proportions of micaceous minerals present in the flakes. Enlargements of typical groups of reflections at about 2.5 Å for a flake from the pallid zone oriented perpendicular to the X-ray beam are presented in Figures 3A and B. Possible assignments for the reflections at ~2.5 Å are listed in Table 1 and were derived by comparison with published XRD patterns of biotite, vermiculite, and kaolinite (see Brown, 1961) and from patterns of K-depleted flakes containing biotite, vermiculite, and mixed-layer biotite-vermiculite obtained in this work. It is evident that the a- and b-axes of biotite, vermiculite, and kaolinite exhibit parallel orientation which is probably inherited from the orientation of these axes in the parent biotite grain. Although unique hk reflections of mixed-layer clay minerals were not noted, these minerals probably retained the orientation of the parent biotite. Nonbasal reflections of gibbsite were not found in these XRD patterns so that the orientation of this mineral remains unknown.

#### *Selected area electron diffraction*

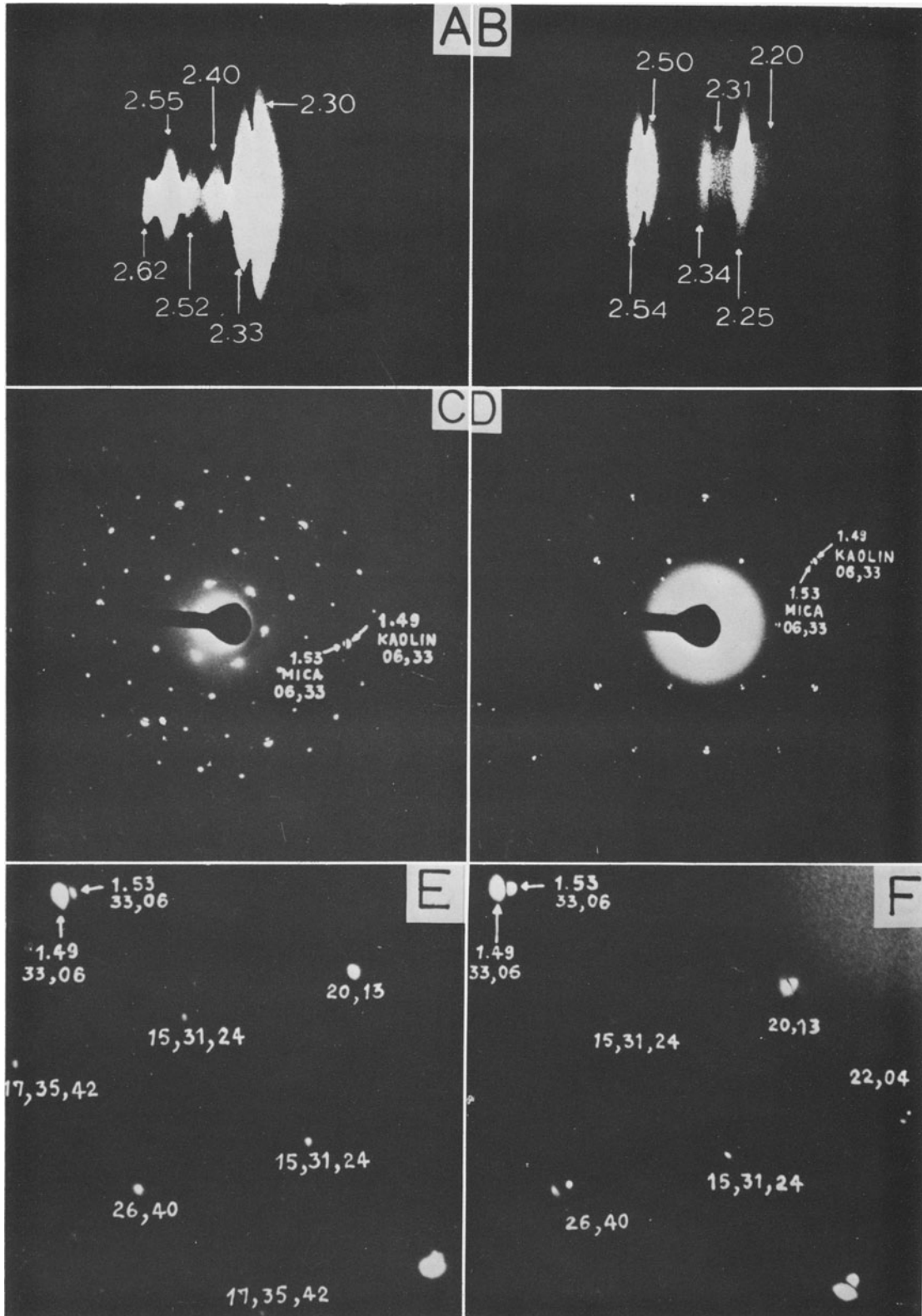
A variety of morphologically distinctive materials are present in scrapings from the surfaces of cleaved, altered biotite grains and may be simply subdivided into micaceous fragments and fine-grained alteration products, although a continuous range of intergrades and mixtures is present. Micaceous fragments with a microcrystalline, mosaic-like morphology are present in scrapings from surfaces of CBD-treated, altered biotite flakes from the pallid zone. These fragments were very susceptible to damage by heating in the electron beam but give characteristic SAD patterns when low beam

Table 1. Indexing of reflections in single grain XRD patterns.

Spacing (Å)	Biotite	Vermiculite	Kaolinite
2.62–2.64	13 $\bar{1}$ , 200	131, 201	—
2.54–2.58	—	134, 202	130, 201
2.48–2.52	131, 20 $\bar{2}$	—	131, 200
2.40–2.45	13 $\bar{2}$ , 201	136, 204	—
2.30–2.34	—	—	131, 20 $\bar{2}$
2.25–2.28	13 $\bar{2}$ , 20 $\bar{3}$	136, 20 $\bar{8}$	—
2.18–2.22	13 $\bar{3}$ , 202	138, 206	13 $\bar{2}$ , 201
2.00	—	208	203, 132

currents are used. The patterns consist of two hk nets of reflections in exact parallel alignment but differ slightly in scale (Figures 3C, D, E, F). The relative intensities of the two patterns varied for different fragments. Accurate measurement of the 060 spacings gave values of 1.53 Å and 1.49 Å indicating the presence of trioctahedral and dioctahedral layer silicates in parallel alignment. The dioctahedral mineral may be kaolinite that had developed epitaxially or topotaxially from a micaceous mineral, thereby adopting the same crystallographic orientation. It is unlikely to be a dioctahedral micaceous mineral since optical, XRD, and electron-optical measurements gave no evidence for the presence of dioctahedral micaceous minerals in these specimens. This interpretation is consistent with the results of XRD studies of single flakes described above which also show a parallelism of the a- and b-axes of kaolinite and micaceous minerals. A greater range of orientations was seen in XRD patterns due to different instrumental factors including the greater angular divergence of the X-ray beam relative to the electron beam. The much greater size of XRD specimens (~10<sup>-4</sup> g) compared to SAD specimens (~10<sup>-13</sup> g) would also have allowed a much greater range of orientations to exist within a single flake.

In contrast to the strong, sharp reflections on well-defined nets present in SAD patterns of micaceous fragments, some fine-grained alteration products gave complex, weak SAD patterns which could rarely be fully interpreted. Minor amounts of 0.1-μm size, raftlike aggregates of laths (~0.05 × 0.005 μm) gave SAD patterns in which the broad, weak reflections mostly fell on regular nets (see Figure 4). Most reflections in this and similar patterns can be indexed on the basis of a goethite unit cell with the Ewald sphere intersecting 0kℓ, 1kℓ, and 2kℓ planes of the reciprocal lattice. The raftlike fragments therefore are parallel arrays of goethite laths resting on their (100) faces so that 0kℓ reciprocal lattice points intersect the Ewald sphere in a region near the center of the pattern. The 1kℓ, 2kℓ reflections may also be the result of undulations within the rafts and elongation of reciprocal lattice points



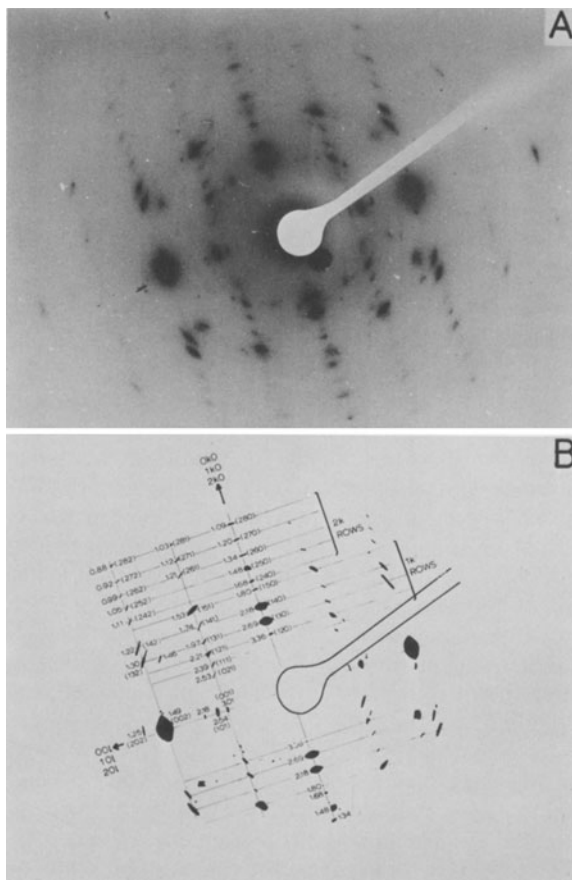


Figure 4. (A) A SAD pattern of a parallel array (raft) of lath-shaped goethite crystals separated from an altered biotite flake from the pallid zone. (B) Spacings in Ångstrom units and indices of the goethite reflections.

along the *a*-axis perpendicular to the laths (Gard, 1971). The arcing of reflections confirms that a range of orientations is present. Although synthetic goethites have generally been found by electron microscopy to consist of well-defined acicular crystals (MacKenzie *et al.*, 1971), natural occurrences of small, lathlike crystals resembling those described here have been reported (Beutelspacher and van der Marel, 1968).

A more complex SAD pattern containing reflections due to goethite and a micaceous mineral is shown in Figure 5A. This specimen consists of a fragment of a micaceous mineral densely coated with hexagonally

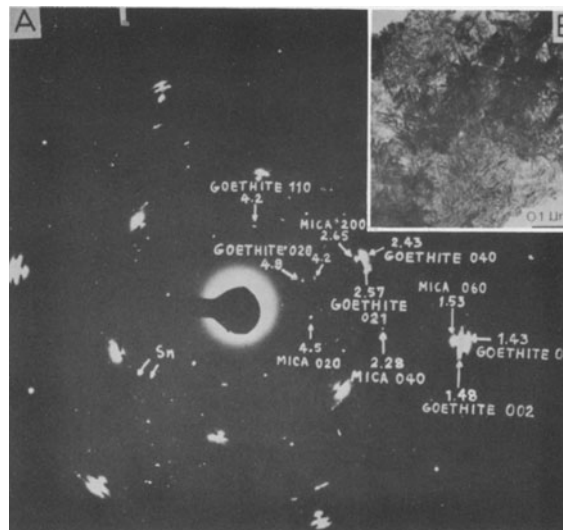


Figure 5. A SAD pattern of a fragment of micaceous mineral coated with hexagonally arranged rafts of goethite crystals (similar to fragment shown in B). Spacings in Ångstrom units. Indices of reflections due to goethite and a trioctahedral micaceous-mineral are shown. Weak rings due to a tin internal standard were visible in the original pattern.

arranged goethite rafts (Figure 5B). The SAD pattern consists of a hexagonally symmetrical net of sharp *hk0* reflections from the micaceous mineral and broader arced goethite *0kℓ* and *1kℓ* reflections. The goethite reflections are also arranged in a hexagonal array since the hexagonal arrangement of rafts on the micaceous substrate has probably resulted in the generation of three goethite patterns at 60° relative rotations. This pattern demonstrates that *c* (goethite) || *b* (mica) and *b* (goethite) || *a* (mica). The same relative orientation of goethite and micaceous mineral was found to exist for many fragments including those in which the goethite rafts were not hexagonally arranged. This result is in direct contrast with the absence of preferred orientation of goethite in whole flakes which was indicated by single flake XRD patterns. The difference may be explained by the optical and electron-optical observations that most goethite occurs as thick, fine-grained deposits rather than as thin layers of hexagonally arranged crystals on micaceous surfaces and by the much smaller size of the regions contributing to SAD patterns.

Figure 3. (A, B) Photographic enlargements of groups of reflections at ~2.5 Å in the XRD pattern of a CBD treated biotite flake from the pallid zone. The XRD pattern was made with the beam normal to the flakes. (C, D) Selected area electron diffraction (SAD) patterns of fragments of mosaic-like micaceous material from a CBD treated altered biotite grain from the pallid zone. (E, F) Photographic enlargements of parts of the patterns in C, D showing the associated *hk* reflections of trioctahedral and dioctahedral minerals. Spacings are indicated in Ångstrom units.

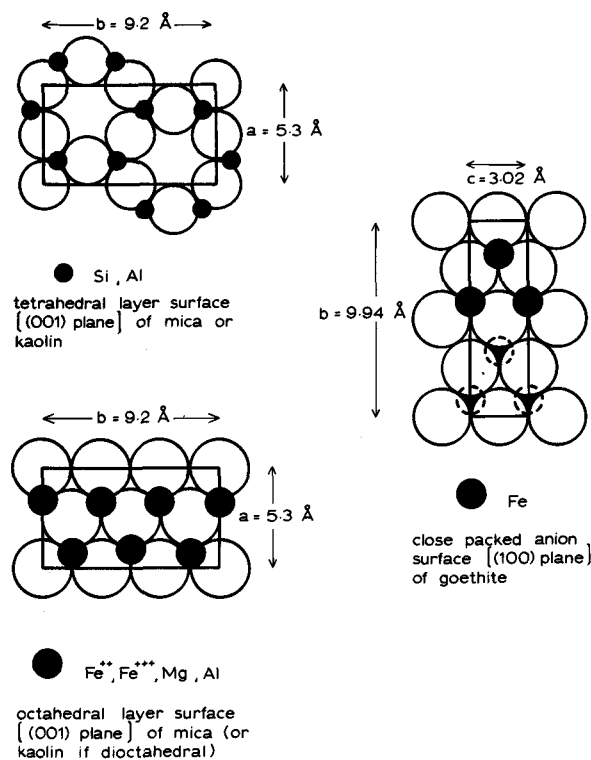


Figure 6. A comparison of the orientation of approximately close-packed anion layers relative to the crystallographic axes of mica, kaolinite, and goethite. The relative orientations of the anion layers shown in this figure are those derived from SAD patterns.

## DISCUSSION

The structure of the parent biotite grain has strongly influenced the orientation of alteration products within the altered biotite pseudomorphs present in saprolite and pallid zones of deeply weathered profiles. Kaolinite has the same orientation as associated micaceous minerals and may have developed by epitaxial or topotaxial replacement. The major differences in structure and chemistry between the kaolinite and the micaceous minerals requires that considerable modification occurred to both cation and anion layers of biotite during this transformation. However, the preserved orientation suggests that some of the approximately close-packed anion layers of the tetrahedral and octahedral sheets have been preserved. If this was the case, silicon and aluminum ions and protons would have migrated through these anion layers to form kaolinite. Magnesium and other cations would have migrated out of the flakes to surfaces where they were released to soil solution. Several mineral alteration processes involve retention of anion layers and diffusion of cations, for example magnetite may alter toptotaxially to maghemite (Sidhu *et al.*, 1977).

The oriented growth of goethite on micaceous mineral surfaces as hexagonal arrangements of lath-shaped crystals is not readily explained as being due to the preservation of close-packed anion layers. The approximately close-packed anion sheets of the (100) surface of goethite and (001) surface of the tetrahedral layer of micaceous minerals are parallel but the axes within these sheets do not coincide, i.e.,  $c$  (goethite) is not parallel to  $a$  (mica). This relationship is depicted in Figure 6. The highly oriented development of goethite on the micaceous mineral surface cannot be regarded as epitaxial growth due simply to continuation of the approximate close packing of this surface. Such an arrangement would lead to parallelism of the  $b$ -axes of the two minerals. However, the goethite close-packed anion sheet may be positioned such that its orientation is the same as that of the anion sheets containing both apical oxygen ions of the silica tetrahedra and hydroxyl ions on the opposite side of the micaceous oxygen surface, i.e., the brucite-like sheet. The relative orientation of micaceous mineral and goethite would then be the same as that deduced from SAD patterns.

Other explanations for the preferred orientation of goethite with respect to the micaceous mineral substrate may be *inter alia* that goethite develops on the hydroxyl surface of a kaolinite interface which has been shown to be highly oriented with respect to biotite. Alternatively goethite crystals may form on correctly oriented nuclei developed from iron-rich regions of the octahedral layer of the micaceous mineral. It is not possible on the basis of the available evidence to determine which of these mechanisms is correct, and possibly all may operate. One clear conclusion is that the structure of the parent biotite grain exerts a strong influence on the development of some kaolinite and goethite in the weathered pseudomorph.

## ACKNOWLEDGMENT

We gratefully acknowledge the assistance of Mr. T. Armitage with the electron microscopy.

## REFERENCES

- Beutelspacher, H. and van der Marel, H. W. (1968) *Atlas of Electron Microscopy of Clay Minerals and their Admixtures*: Elsevier, New York, 333 pp.
- Brown, G., ed. (1961) *The X-ray Identification and Crystal Structures of Clay Minerals*: Mineralogical Society, London, 544 pp.
- Eswaran, H. and Bin, W. C. (1978) A study of a deep weathering profile on granite in Peninsula Malaysia: III: Alteration of feldspars: *Soil Sci. Soc. Amer. J.* **42**, 154–158.
- Eswaran, H. and Heng, Y. Y. (1976) The weathering of biotite in a profile on gneiss in Malaysia: *Geoderma* **16**, 9–20.
- Gandolfi, G. (1967) Discussion upon methods to obtain X-ray powder patterns from a single crystal: *Mineral. Petrogr. Acta* **13**, 67–74.
- Gard, J. A. (1971) Interpretation of electron micrographs and electron-diffraction patterns: in *The Electron-Optical In-*

- Investigation of Clays*, J. A. Gard, ed., Mineralogical Society, London, 27–79.
- Gilkes, R. J. and Suddhiprakarn, A. (1979) Biotite alteration in deeply weathered granite. I. Morphological, mineralogical and chemical properties. *Clays & Clay Minerals* **27**, 349–360.
- Hendricks, S. B. (1940) Variable structures and continuous scattering of X-rays from layer-silicate lattices: *Phys. Rev.* **57**, 448–454.
- MacEwan, D. M. C. (1961) Montmorillonite minerals: in *The X-ray Identification and Crystal Structures of Clay Minerals*, G. Brown, ed., Mineralogical Society, London, 143–208.
- MacKenzie, R. C., Follett, E. A. C., and Meldau, R. (1971) The oxides of iron, aluminium and manganese: in *The Electron-Optical Investigation of Clays*, J. A. Gard, ed., Mineralogical Society, London, 315–348.
- Sidhu, P. S., Gilkes, R. J., and Posner, A. M. (1977) Mechanism of the low temperature oxidation of synthetic magnetites: *J. Inorg. Nucl. Chem.* **39**, 1953–1958.
- (Received 3 October 1978; accepted 7 June 1979.)

**Резюме**—Рентгеновские и электронно-дифракционные картины одиночных зерен выветренных чешуек биотита выявили группирование отражений 00l и hk биотита, вермикулита, смешанно-слоистых глинистых минералов, и каолинита, показывающие, что вторичные минералы находятся в параллельной кристаллографической ориентации к материнскому биотиту. Астеризм биотитовых отражений усиливается в результате выветривания. Кристаллы гиббсита выросли в параллельной базальной ориентации к чешуйкам биотита. Большинство гетита в выветренном биотите находится в виде агрегатов беспорядочно ориентированных кристаллов в кливаже и на поверхностях зерен. Часть гетита присутствует на обломках слюды в виде лейстовидных кристаллов размером 0,05  $\mu\text{m}$  в гексагональной упаковке с гранью (100), расположенной на биотитовой грани (001). Электронно-дифракционные картины выбранной зоны агрегатов лейстовидных кристаллов гетита содержат отражения  $0k\ell$ ,  $1k\ell$ , и  $2k\ell$  благодаря ундуляции агрегатов и чрезвычайной тонкости кристаллов. Эти картины показывают, что близко расположенные анионные слои в гетите совпадают с бруситоподобным слоем слюдистых минералов.

**Resümee**—Einkristallröntgenaufnahmen und Elektronenbeugungsdiagramme der verwitterten Biotitblättchen zeigen Gruppierungen der 00l- und hk-Reflexe von Biotit, Vermiculit, Wechsellagerungen, und Kaolinit, die erkennen lassen, daß die sekundären Minerale parallel zum Ausgangsbiotit orientiert sind. Asterismen der Biotitreflexe werden durch die Verwitterung verstärkt. Gibbsitkristalle sind parallel zur Basis der Biotitblättchen orientiert. Ein großer Teil des Goethit in den verwitterten Biotiten kommt in Form von Aggregaten aus regellos angeordneten Kristallen auf Spaltflächen und auf Kornoberflächen vor. Einige Goethite treten auf den Glimmerresten als leistenförmige 0,05  $\mu\text{m}$  große Kristalle in hexagonaler Anordnung auf, wobei ihre (100)-Fläche auf der (001)-Fläche des Biotit aufliegt. Feinbereichselektronenbeugungsdiagramme der Aggregate aus leistenförmigen Goethitkristallen enthalten  $0k\ell$ -,  $1k\ell$ -, und  $2k\ell$ -Reflexe, die von Unregelmäßigkeiten der Aggregate und von der außerordentlich geringen Dicke der Kristalle herrühren. Diese Diagramme deuten darauf hin, daß die dicht besetzten Anionschichten des Goethit mit der Brucit-Schicht der glimmerartigen Minerale zusammenfallen.

**Résumé**—Les clichés de diffraction d'électrons et ceux de rayons-X de grains simples de lames altérées de biotite montrent des groupements (00l) et des réflexions hk de biotite, de vermiculite, de minéraux argileux à couches mélangées, et de kaolinite indiquant que les minéraux secondaires sont cristallographiquement parallèles à la biotite-mère. L'astérisme des réflexions de biotite est augmenté par l'altération. Des cristaux de gibbsite se sont développés dans une orientation de base parallèle aux lames de biotite. La plupart de la goethite dans la biotite altérée existe en agrégats de cristaux orientés au hasard dans des fendages et sur les surfaces des grains. Sur des fragments micacés, la goethite est présente comme cristaux en forme de latte de 0,05  $\mu\text{m}$  en arrangement hexagonal avec leur face (100) reposant sur la face de biotite (001). Des clichés de diffraction d'électrons de régions sélectionnées d'agrégats de cristaux de goethite en forme de latte contiennent des réflexions  $0k\ell$ ,  $1k\ell$ , et  $2k\ell$  à cause d'ondulations des agrégats et de l'extrême minceur des cristaux. Ces clichés indiquent que les couches d'anions fortement rapprochées l'une de l'autre dans la goethite coïncident avec la couche semblable à la brucite des minéraux micacés.